Magazine of Civil Engineering

ISSN 2712-8172

journal homepage: http://engstroy.spbstu.ru/

DOI: 10.34910/MCE.110.14

Performance of elastomeric seismic isolators under long-period earthquakes

O. Abrar ***  **, *S. Tuhta

Department of Civil Engineering, Ondokuz Mayis University, Samsun, Turkey

**E-mail: obaidullah.abrar@gmail.com*

Keywords: earthquake engineering, seismic isolation, elastomeric isolator, finite element method, long-period earthquake, nonlinear analysis

Abstract. This research investigates the performance of elastomeric (laminated rubber) seismic isolators for the protection of medium-rise structures under the effect of long-period earthquakes. A finite element model of a midrise structure with elastomeric seismic isolators has been modeled and the dynamic performance of the structure has been examined under the effect of the 1985 Michoacán (Mexico City), 2003 Tokachi-Oki, 2010 El Mayor, and the 2016 Kaikoura earthquakes. The performance of the structure is studied in three cases, all equipped with elastomeric isolators with different natural periods. The natural-period of isolators in the first, second, and third cases is 2.5, 4, and 5 seconds, respectively. The comparison of the three cases in terms of mitigating earthquake energy shows that the effectiveness of elastomeric seismic isolators with lower periods (2–3 seconds) is significantly limited under the effect of long-period earthquakes. In common practice, elastomeric seismic isolators are produced and used with a natural period of 2–3 seconds, a seismic isolator having a period within the mentioned range will have serious shortcomings for dissipating earthquake energy when subjected to a long-period earthquake. The results of this study indicate that elastomeric seismic isolators with 5-seconds exhibited considerably better performance compared to that of 2.5 and 4-second seismic isolators.

1. Introduction

Seismic base isolation is considered a reliable technique for the protection of structures under effect strong ground motions, general idea of seismic isolation is to increase the natural period of structure to a point that enables the structures to safely overcome the harmful effect of an earthquake. Elastomeric seismic isolators (e.g. laminated rubber bearing, lead rubber bearing, high damping rubber bearing, etc.) are among the most commonly used seismic isolation devices which are produced with a 2 to 3 seconds natural period [1, 2]. However, based on earthquake event reports the effectiveness of elastomeric seismic isolators considerably diminishes when subjected to a long-period earthquake (a ground motion with a longer period which does not fall within the range of the mentioned elastomeric isolator period), for instance, there have been serious damages in the seismic isolation devices of buildings under the long-period effect of the 2011 Tohoku earthquake [3]. The relatively short natural period of these seismic isolation devices is dominated by the longer period of the long-period earthquake and as a result of it, the story acceleration of the structure will not be dissipated as much as expected for a seismic isolated structure, eventually, the seismic isolator will fail in severe cases due to large displacements (exceeding the displacement limit of the elastomeric isolators) [4].

The harmful effect of long-period earthquakes has long been observed in seismically active regions several times, long-period earthquakes are generated due to rupture propagation and wave radiation in near-field ground motions. It is also generated due to seismic wave amplification in a distant sedimentary soft-soil basin and it imposes a serious threat to structures located far from the epicenter of the earthquake [5]. 1985 Michoacán, 1999 Chi-chi, 2003 Tokachi-Oki, 2010 El Mayor, 2011 Tohoku, 2016 Kaikoura

Abrar, O., Tuhta, S. Performance of elastomeric seismic isolators under long-period earthquakes. Magazine of Civil Engineering. 2022. 110(2). Article No. 11014. DOI: 10.34910/MCE.110.14

earthquakes are noted as the worst examples of the long-period ground motions [5–9]. The 2011 Tohoku earthquake generated a long-period earthquake affecting much of the east coast of Japan, tall buildings have been subjected to large displacement due to the long-period effect of the earthquake. For instance, a 52-floor building in Osaka located 770 km from the epicenter of the earthquake had a 1.32 m displacement, Osaka region has a dominant period of 6 seconds which correlates with the dominant period of the long-period earthquake that happened in the sedimentary soil layers of Osaka region [3].

In the literature, there are several studies regarding the enhancement of seismic base isolation systems, different methods are used to improve the performance of seismic isolation. Ismail et al. proposed a novel seismic isolation device equipped with a mechanism to effectively dissipate the near-fault pulse-like earthquakes [10]. Kasimzade et al. developed a seismic isolation system that intends to provide a longer period for the structures for improving the overall performance of important structures against near-fault and long-period earthquakes [11, 12]. Herbut suggests the usage of a wave generator in the soil-foundation boundary of the structure to reduce the amplitude of ground motion [13]. Tavakoli et al. examined the performance of fixed-base and seismically isolated buildings under the effect of far-field and near-fault ground motions [14]. Plenty of studies on seismic base isolation are focused on short-period and short-duration ground motions [15–18]. On the other hand, few studies are dedicated to the effect of the long-period earthquakes on seismic isolated structures and are focused on special structures such as oil tanks and bridges [19, 20].

This paper investigates the performance of low-period (2.5 seconds) elastomeric seismic isolation (laminated rubber bearing) devices in comparison with a figurative seismic isolator with a longer period (4 and 5 seconds) for protection of a 4-story building against the effect of long-period earthquakes. The finite element model of a 4-story seismically isolated structure has been prepared in a manner that the superstructure and the seismic isolators exhibit linear and nonlinear behaviors respectively. The dynamic finite element model has been solved using LS-DYNA explicit solver under the effect of the 1985 Mexico City, 2003 Tokachi-Oki, 2010 El Mayor, and the 2016 Kaikoura earthquakes.

2. Method

2.1. Model Description

A finite element model of a 4-story building (Fig. 1) with a system of laminated rubber seismic isolators has been prepared. The model consists of 36 columns each laying on a seismic isolator, the isolators are positioned on a raft foundation. One-dimensional beam elements (Hughes Liu) are used to model the columns and beams of the superstructure, for modeling the foundation and the bases of the columns 8-node constant stress solid element is used. All parts of the structure are modeled using elastic material (C30 concrete), except for the seismic isolators which are modeled using a special material, the nonlinear seismic isolator which exhibits hysteresis behavior.

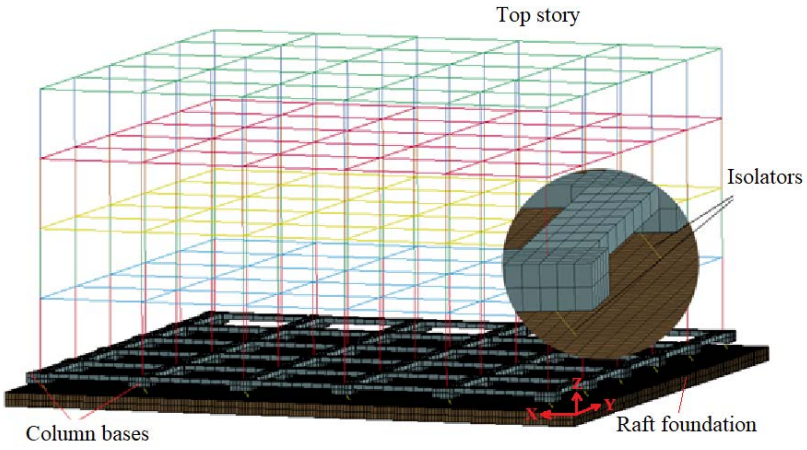

Figure 1. Finite element model of the 4-story seismic isolated structure.

Seismic isolators are modeled using a single discrete beam element which has the capability of representing an elastomeric isolator. The general properties of the seismic isolators are calculated based on the building and its soil characteristics and the calculated seismic isolator parameters are assigned to the respective beam element. The properties of the seismic isolator are modeled by considering the bidirectionally coupled plasticity theory which satisfies the nonlinear hysteresis behavior proposed by Wen [21]. The algorithm for solving the nonlinear seismic isolator was developed by Nagarajaiah et al [22]. The general representation of the equation of motion (equation 1) and the nonlinear formulation (equation 2) of the seismic isolation system are presented as follows.

$$[m]\{\ddot{u}\}+[c]\{\dot{u}\}+[k]\{u\}+[L]\{f_r\}=-[m]\{e\}\{\ddot{u}_g\}, \tag{1}$$

$$f_r = c_b\dot{u}_b + \alpha k_b u_b + (1-\alpha)\, f_y Z, \tag{2}$$

$$\dot{Z} = \left[Au_b - \beta |\dot{u}_b| Z |Z|^{n-1} - \tau\dot{u}_b |Z|^n \right] u_y^{-1}. \tag{3}$$

Here, m, c, k, $\ddot{u}$, $\dot{u}$, and u are the mass, damping, stiffness matrices, acceleration, velocity, and displacement vectors of the model respectively. The matrix L refers to the location of isolators and f_r represents the nonlinear hysteresis restoring force of the isolator which satisfies Wen's nonlinear model. $\ddot{u}_g$ is the acceleration vector of ground motion and the vector e refers to the influence coefficient of displacement transformation respective to each degree of freedom. k_b, c_b, u_b, $\dot{u}_b$, f_y, and u_y are the stiffness, damping, displacement, velocity, yield force, and yield displacement components of the seismic isolator respectively. α refers to the ratio of the post-yield to pre-yield stiffness of the seismic isolator. Z is the non-dimensional hysteresis displacement component of Wen's nonlinear model and can be presented via equation (3). A, β, and τ are dimensionless parameters of the isolator that are determined based on experimental tests. n is a constant which controls the smoothness of transition from elastic to the plastic response.

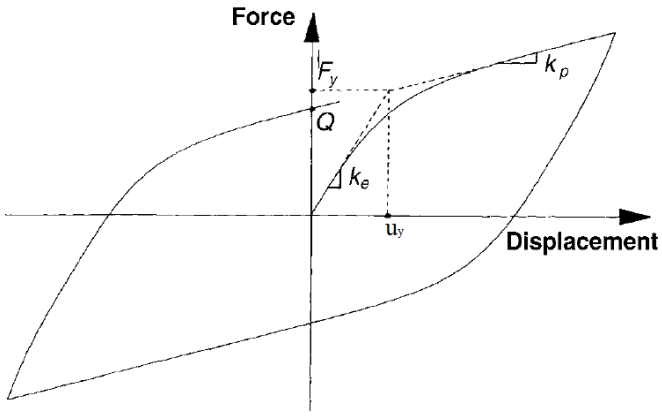

Figure 2. Hysteresis restoring force-displacement curve of seismic isolator.

2.2. Properties of Isolators

The properties of the laminated rubber seismic isolators are calculated based on the characteristics of the structure and the properties of the soil on which the structure is going to be built. There are various codes and regulations for the calculation of the properties of the seismic isolators. In this study, the standard published by the American Society of Civil Engineers (ASCE 7-10 and ASCE 41-13) has been used [23], [24]. Vertical stiffness (k_v), yield force (f_y), and yield displacement (u_y) of the isolator is calculated as three cases depending on the selected period of the isolator (T_D) using the following equations.

$$K_{D\min} = \frac{4\pi^2 W}{T_D^2 g}, \tag{4}$$

$$D_D = \frac{gS_{D1}T_D}{4\pi^2 B_D}. \tag{5}$$

Here, W is the weight of structure imposed on a single seismic isolator, K_b, B_D, and D_D are the horizontal stiffness, damping coefficient, and design displacement of the isolator respectively. S_{D1} is the spectral response acceleration parameter of the ground motion and g is the gravitational acceleration. The sectional area (A_r) and the post-yield stiffness (K_p) of the rubber bearing are calculated based on equations (6) and (7) respectively.

$$A_r = \frac{K_D t_r}{R_T}, \tag{6}$$

$$K_p = \frac{GA_r f_L}{R_T}, \tag{7}$$

where t_r is the thickness of a single rubber layer separated by steel sheet, G is the shear modulus of the rubber, and R_T is the total rubber thickness and f_L is a factor commonly taken as 1.5. Experimentally, yield displacement (u_y) is calculated as 0.05 – 0.1 times of R_T. The characteristic-strength of the isolator is calculated using equation (8), using the described parameters the yield force of the isolator is calculated by equation (9).

$$u_y = \frac{Q}{5.5K_p}, \tag{8}$$

$$F_y = Q + K_p u_y. \tag{9}$$

Having the above parameters, the vertical stiffness (K_v) of the isolator is calculated using equation (10).

$$K_V = \frac{\left(E_c A_r\right)}{R_T}, \tag{10}$$

$$E_c = \frac{6GS^2K}{6GS^2 + K}. \tag{11}$$

Equation (11) is used to calculate the elasticity modulus of the rubber-steel composite which is bonded under specific heat and pressure. K is the bulk modulus of the rubber, the value of the K and G varies for different rubber compounds, it varies 1000 – 2500 MPa and 0.45 – 1 MPa respectively [1]. S is a factor that refers to the shape of the hysteresis loop of the elastomeric isolator, ideally, it ranges between 12 – 20. In accordance with the presented equations, the properties of the laminated rubber seismic isolators are calculated and presented in Table 1.

Table 1. Properties of computed laminated rubber seismic isolators.

Parameters	T_D: 2.5 s	T_D: 4 s	T_D: 5 s
K_v (N/m)	2.674E+09	8.884E+08	6.249E+08
K_b (N/m)	1.793E+06	7.002E+05	4.481E+05
F_y (N)	1.165E+05	9.103E+04	7.282E+04
u_y (m)	0.01	0.02	0.025
R_T (m)	0.2	0.4	0.5

2.3. Numerical Analysis

The performance of presented seismic isolators for mitigation of ground motion accelerations in the 4-story building is investigated under the effect of five earthquake ground motions as provided in Table 2 and Fig. 3. The ground motion accelerations records are obtained from the Virtual Data Center (VDC) [25] and Pacific Earthquake Engineering Research Center (PEER) ground motion record databases [26].

Table 2. List of earthquakes used in numerical analysis.

Earthquake	Year	M_w	Station	PGA (m/s^2)	PGD (cm)	Hypo-central Distance (km)
Michoacán, Mexico	1985	8.1	La Union	1.6	7.10	83.9
El Mayor, USA/Mexico	2010	7.2	El Centro Array 11	5.7	39.7	61.8
El Mayor, USA/Mexico	2010	7.2	Chihuahua	2.4	44.7	25.7
Tokachi Oki, Japan	2003	8.3	Kushiro Gov. Building	2.6	15.7	136.1
Kaikoura, New Zealand	2016	7.8	Seddon Fire Station	7.1	20.7	145.3

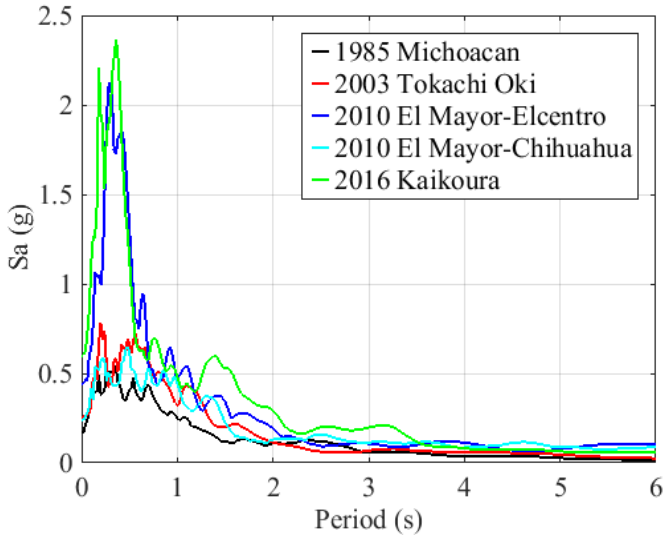

Figure 3. The spectral acceleration of earthquake excitations used in numerical analysis.

For conducting finite element nonlinear dynamic analysis, LS-DYNA explicit solver code has been used, each analysis required 5-10 hours varying based on the duration of ground motion excitation. A computer with a capacity of 16 CPU cores and 32 GB of RAM has been used to conduct the respective dynamic analyses.

3. *Results and Discussion*

The top story acceleration, top story displacement of the building, and the nonlinear hysteresis force-displacement responses of seismic isolators with different periods (2.5s, 4.0s, and 5s) have been obtained and presented comparatively via Fig. 4-8.

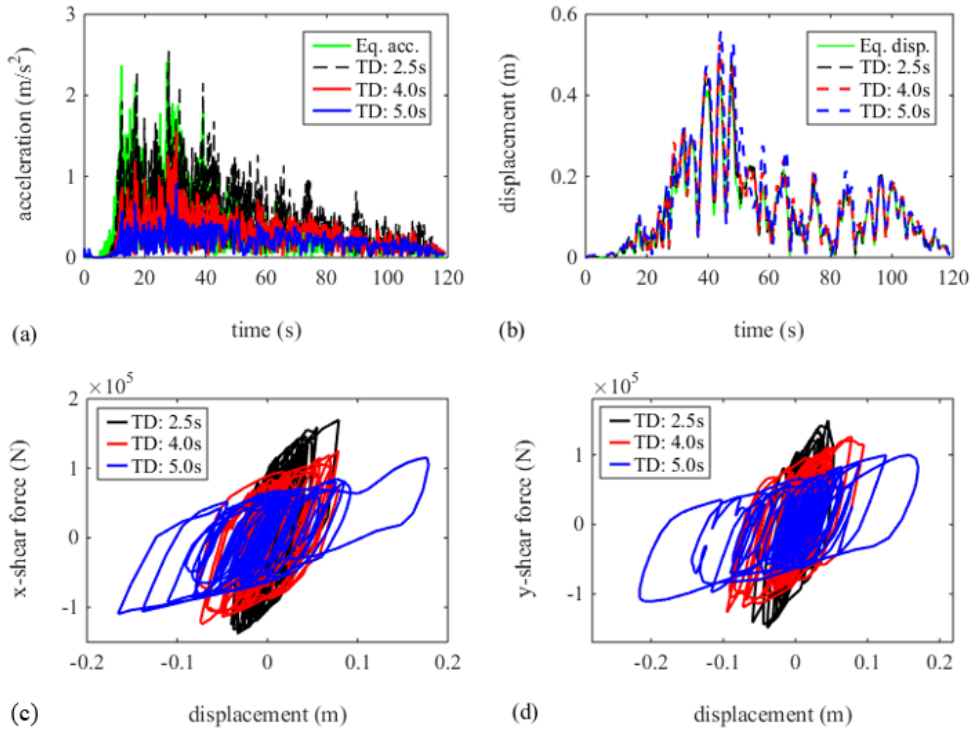

Figure 4. El Mayor-Chihuahua (2010) response: (a) top story acceleration, (b) top story displacement, (c) and (d) hysteresis force-displacement curve in x and y directions respectively.

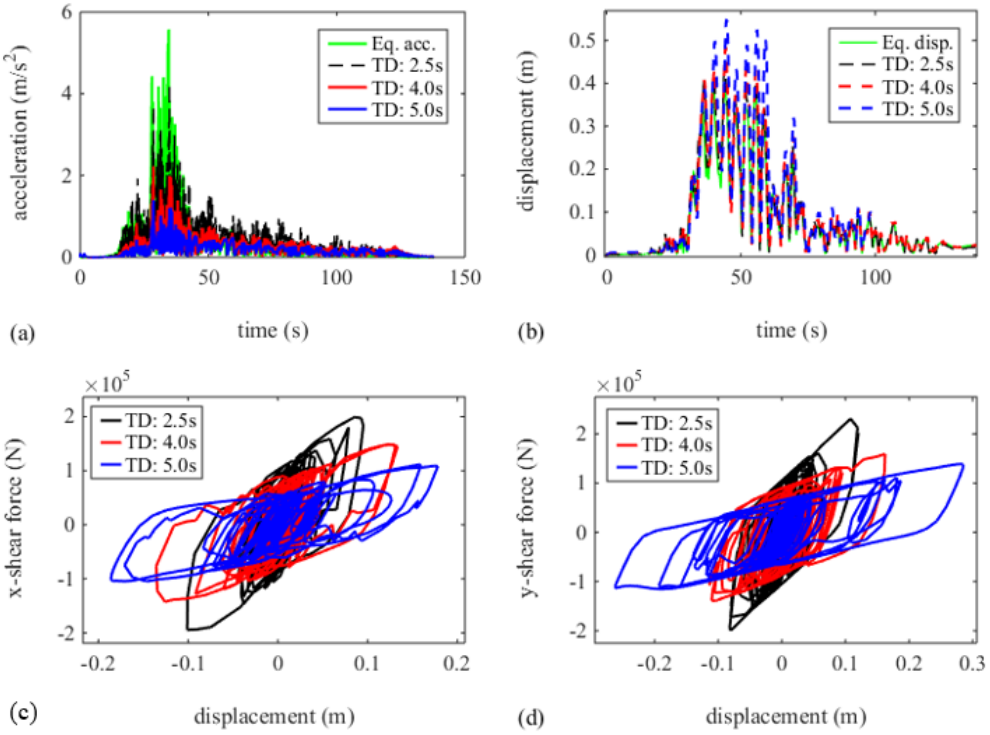

Figure 5. El Mayor-El Centro (2010) response: (a) top story acceleration, (b) top story displacement, (c) and (d) hysteresis force-displacement curve in x and y directions respectively.

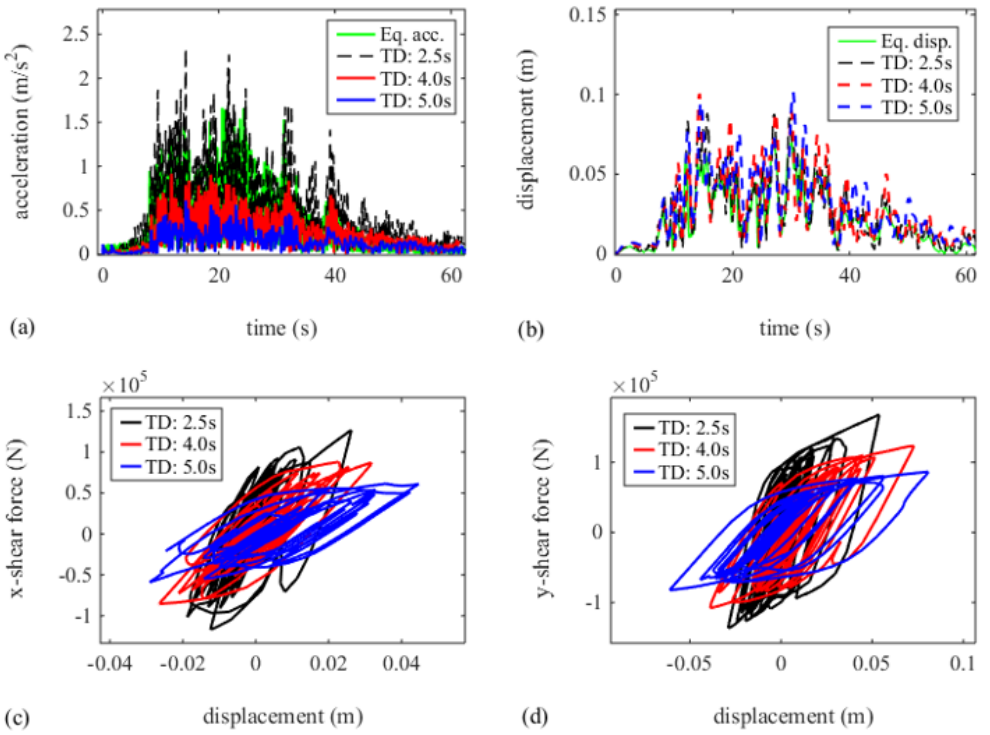

Figure 6. Michoacán (1985) response: (a) top story acceleration, (b) top story displacement, (c) and (d) hysteresis force-displacement curve in x and y directions respectively.

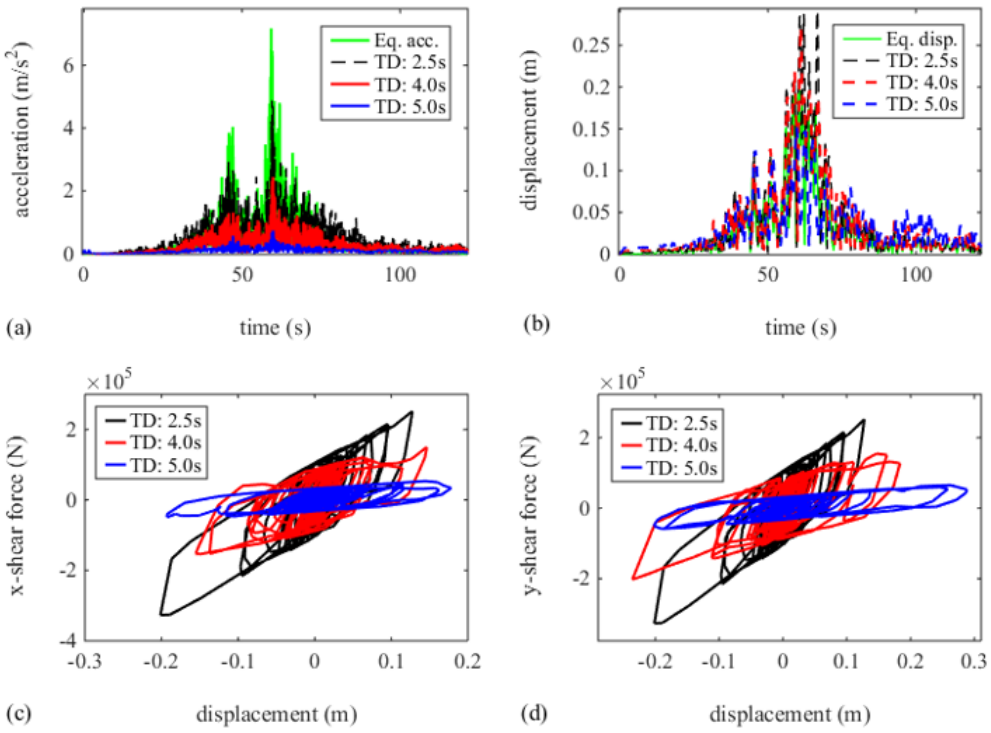

Figure 7. Kaikoura (2016) response: (a) top story acceleration, (b) top story displacement, (c) and (d) hysteresis force-displacement curve in x and y directions respectively.

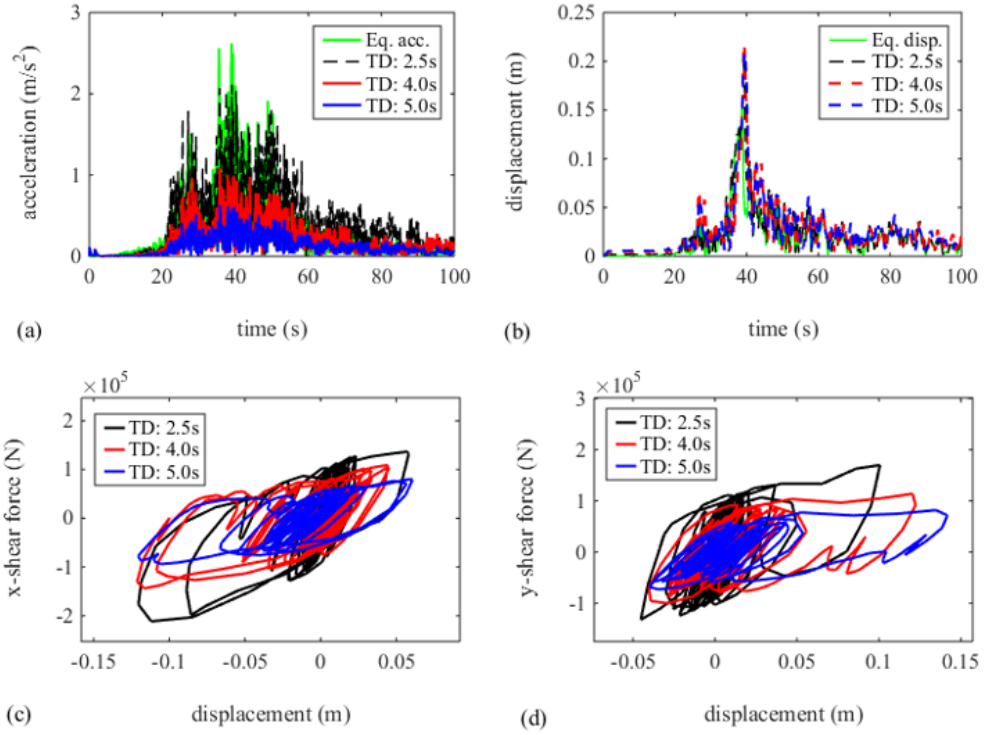

Figure 8. Tokachi-Oki (2003) response: (a) top story acceleration, (b) top story displacement, (c) and (d) hysteresis force-displacement curve in x and y directions respectively.

Top story acceleration results indicate that the response of seismic isolators with 4s and 5s-period is significantly lower than the 2.5s-period isolator, the top story acceleration response has relatively decreased by increasing the period of the isolator as presented in Fig. 4a, 5a, 6a, 7a, and 8a. The reduction in acceleration response of the superstructure is due to the reason that longer period of the 5s and 4s-period isolator, in this case, the isolator has more elasticity and has the capability of larger displacement compared to that of the 2.5s-period isolator. The hysteresis force-displacement behavior of the isolator implies that 5s and 4s-period isolator had larger displacement compared to that of the 2.5s-period isolator, meanwhile, the shear force on the isolators have dropped significantly as shown in Fig. 4c, 4d, 5c, 5d, 6c, 6d, 7c, 7d, 8c, and 8d.

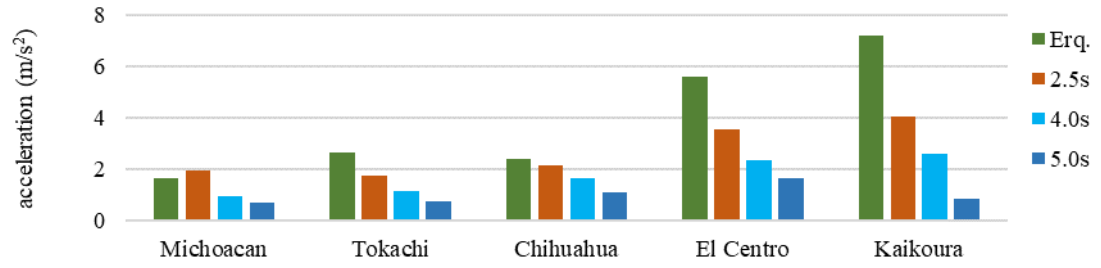

Figure 9. Comparison of top story acceleration response of the model under respective earthquakes.

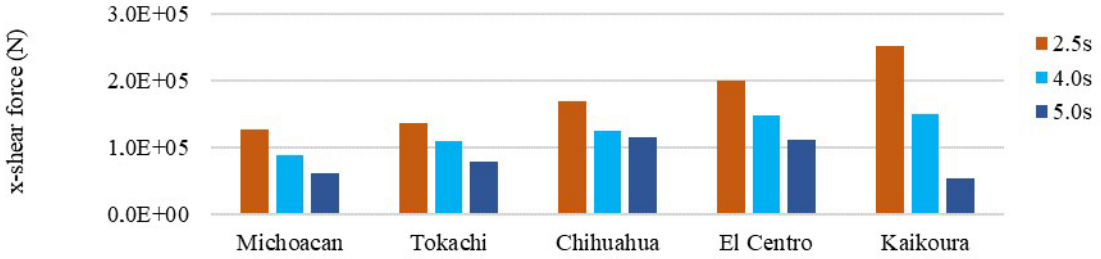

Figure 10. Comparison of shear force response of isolators under respective earthquakes in the x-direction.

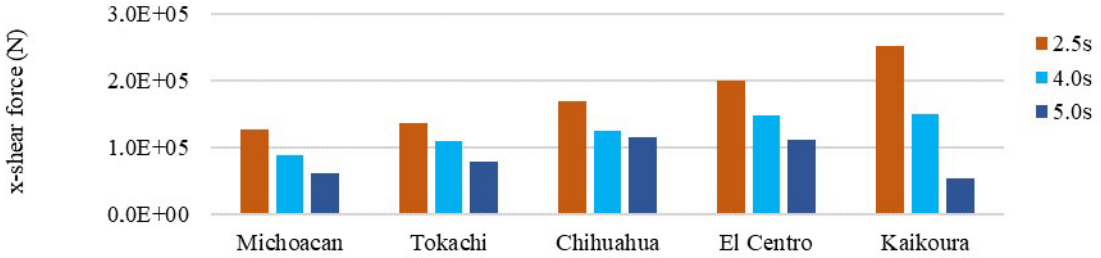

Figure 11. Comparison of shear force response of isolators under respective earthquakes in the x-direction

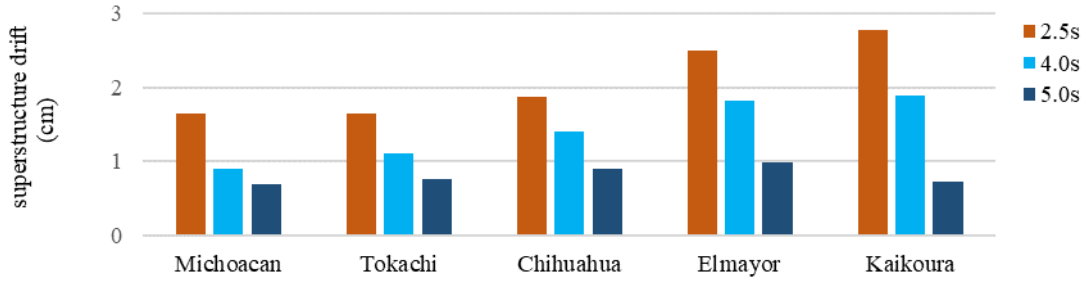

Figure 12. Comparison of superstructure drift under the effect of respective earthquakes.

Overall, the acceleration response of the top story of the structure has decreased by 35.65 % and 60.54 % for 4s and 5s-period isolator respectively in comparison with the 2.5s-period seismic isolator as shown in Fig. 9. Similarly, the base shear in the seismic isolator with 4s and 5s-period have decreased by 28.80 % and 49.50 % respectively in comparison with the 2.5s-period seismic isolator as presented in Fig. 10 and 11. The story drift of the model under the effect of respective earthquakes is shown in Fig. 12, similar to the acceleration and base shear response, the story drift has decreased in 4 and 5s-period seismic isolators in comparison with the 2.5s-period isolator.

The design of an elastomeric seismic isolator with a 5s-period and above requires a deep study on the materials that are used in the production of elastomeric isolators. Usage of highly resilient rubber compounds with highly durable materials (e.g. carbon fiber) as shims is an option for the design of such isolators, and it is a topic for future studies.

4. Conclusion

In this study, the seismic performance of three different elastomeric (laminated rubber) seismic isolators with different natural periods has been studied comparatively. Dynamic analysis of the seismic isolated structure has been conducted under the effect of five long-period earthquakes. The outcome of the study can be concluded as follows:

1. The earthquake mitigation performance of commonly produced elastomeric seismic isolators (with 2-3s-period) is significantly low under the effect of long-period earthquakes; it could lead to failure of the seismic isolators due to the concentration of shear force on seismic isolators.

2. For inhibition of long-period earthquakes a seismic isolator with a longer natural period is required that could allow larger displacement capabilities.

3. Increasing the period of elastomeric isolators to 4-5 s has considerably increased the effectiveness of the elastomeric isolators in terms of dissipating the energy of earthquakes in the top stories of the superstructure.

4. The shear-force on seismic isolators has been decreased relatively with increasing the period of the seismic isolators, 5-second period isolator has the lowest shear force response.

5. The isolator model with 4 and 5s- period can be used as a reference to be implemented in the protection of buildings in regions with the high possibility of occurring long-period ground motions which can impose serious threats to buildings equipped with conventionally implemented elastomeric seismic isolators with a 2-3s period.

References

1. Naeim, F. The Seismic Design Handbook. 1. New York, Springer, 2001. ISBN: 978-1-4613-5681-3
2. Ozden, B. LOW-COST SEISMIC BASE ISOLATION USING SCRAP TIRE PADS (STP). MSc. Ankara - Turkey, Middle East Technical University, 2006.
3. Saito, T. Behavior of response controlled and seismically isolated buildings during severe earthquakes in Japan. Energy, Environment and Innovation Magazine. 2015. Pp. 31–37.
4. Jangid, R.S. Optimum friction pendulum system for near-fault motions. Engineering Structures. 2005. 27(349–359). DOI: https://doi.org/10.1016/j.engstruct.2004.09.013
5. Kazuki, K., Hiroe, M.A. A seismological overview of long-period ground motion. Journal of Seismology. 2008. 12(2). Pp. 133–143. DOI: https://doi.org/10.1007/s10950-007-9080-0
6. Bozorgnia, Y., Bertero, V.V. Earthquake Engineering: From Engineering Seismmology to Performance-Based Engineering. Washington D.C., CRC Press LLC, 2004. ISBN: 0-203-48624-2.
7. Duputel, Z., Rivera, L. Long-period analysis of the 2016 Kaikoura earthquake. Physics of the Earth and Planetary Interiors. 2017. 265(April). Pp. 62–66. DOI: 10.1016/j.pepi.2017.02.004
8. Hall, J.F., Heaton, T.H., Halling, M.W., Wald, D.J. Near-source ground motion and its effects on flexible buildings. Earthquake Spectra. 1995. 11(4). Pp. 569–605. DOI: https://doi.org/10.1193/1.1585828
9. Loh, C.H., Wu, T.C., Huwang, N.E. Application of the empirical mode decomposition – Hilbert spectrum method to identify near-fault ground-motion characteristics. Bulletin of the Seismological Society of America. 2001. 9(5). Pp. 1339–1357. URL: https://pdfs.semanticscholar.org/7d25/84484237712d714539f34324048bd3611cdf.pdf
10. Ismail, M., Rodellar, J., Ikhouane, F. Performance of structure–equipment systems with a novel roll-n-cage isolation bearing. Computers & Structures. 2009. 87(23–24). Pp. 1146–1631. DOI: https://doi.org/10.1016/j.compstruc.2009.09.006
11. Kasimzade, A.A., Abrar, O., Atmaca, G., Kuruoglu, M. New structural seismic protection for high-rise building structures. Journal of Vibroengineering. 2020. 22(4). Pp. 831–848. DOI: doi.org/10.21595/jve.2019.20741
12. Kasimzade, A.A., Abrar, O., Kuruoglu, M., Atmaca, G. New Structural Seismic Isolation for Nuclear Containment Structures. Science and Technology of Nuclear Installations. 2020. 2020(9573653). Pp. 1–15. DOI: doi.org/10.1155/2020/9573653
13. Herbut, A. A proposal for vibration isolation of structures by using a wave generator. Soil Dynamics and Earthquake Engineering. 2017. 100. Pp. 573–585. DOI: https://doi.org/10.1016/j.soildyn.2017.07.005
14. Tavakoli, H.R., Naghavi, F., Goltabar, A.R. Dynamic Reponse of the Base-Fixed and Isolated Building Frames Under Far and Near-Fauld Earthquakes. Arabian Journal of Science and Engineering. 2014. 39. Pp. 2573–2585. DOI: 10.1007/s13369-013-0891-8
15. Han, J., Kyu, M., Choi, I. Experimental study on seismic behavior of lead-rubber bearing considering bi-directional horizontal input motions. Engineering Structures. 2019. 198(August). Pp. 2019.
16. Jian, F., Xiaohong, L., Yanping, Z. Optimum design of lead-rubber bearing system with uncertainty parameters. Structural Engineering and Mechanics. 2015. 56(6). Pp. 959–982.
17. Pradip, D.J., Sunila, G., Dume, S.M. Earthquake performance of RC Buildings using Elastomeric Base Isolation Controls. International Journal of Engineering Research and Applications. 2013. 3(6). Pp. 1518–1524.
18. Shoaei, P., Tahmasebi, H., Mehdi, S. Seismic reliability-based design of inelastic base-isolated structures with lead-rubber bearing systems. Soil Dynamics and Earthquake Engineering. 2018. 115(June). Pp. 589–605.
19. Anajafi, H., Poursadr, K., Roohi, M., Santini-Bell, E. Effectiveness of Seismic Isolation for Long-Period Structures Subject to Far-Field and Near-Field Excitations. 2020. 6(24). DOI: 10.3389/fbuil.2020.00024.
20. Cheng, X., Jing, W., Li, D. Dynamic response of concrete tanks under far-field, long-period earthquakes. Proceedings of the Institution of Civil Engineers – Structures and Buildings. 2019. Pp. 1–14. DOI: 10.1680/jstbu.18.00024.

21. Wen, Y.K. Method for Random Vibration of Hysteretic Systems. Journal of Engineering Mechanics. 1976. 102(2). Pp. 249–264.
22. Nagarajaiah, S., Reinhorn, A.M., Constantinou, M.C. Nonlinear Dynamic Analysis of 3-D-Base-Isolated Structures. Journal of Structural Engineering. 1991. 117(7). Pp. 2035–2054. DOI:doi.org/10.1061/(ASCE)0733-9445(1991)117:7(2035).
23. ASCE 7-16. Minimum Design Loads for Buildings and Other Structures. Reston, American Society of Civil Engineers, 2016.
24. ASCE 41-13. Seismic Evaluation and Retrofit of Existing Buildings. Reston, American Society of Civil Engineers, 2013.
25. VDC. Storng-Motion Virtual Data Center. USGS, 2020. URL: https://www.strongmotioncenter.org/vdc/scripts/earthquakes.plx
26. PEER. PEER Strong Ground Motion Database. Berkeley University, 2018. URL: https://ngawest2.berkeley.edu/

Contacts:

Obaidullah Abrar, obaidullah.abrar@gmail.com
Sertac Tuhta, stuhta@omu.edu.tr

Received 08.02.2021. Approved after reviewing 06.04.2021. Accepted 07.04.2021.